Institute of
Applied Mechanics
Institut für Baumechanik

Graz University of Technology

Preprint Series

Institute of Applied Mechanics

Graz University of Technology

Preprint No 1/2009

On a reformulated Convolution Quadrature based Boundary Element Method

Martin Schanz
Institute of Applied Mechanics, Graz University of Technology

Published in: *Computer Modeling in Engineering & Sciences*, 58(2), 109–128, 2010

Latest revision: March 20, 2010

Abstract

Boundary Element formulations in time domain suffer from two problems. First, for hyperbolic problems not too much fundamental solutions are available and, second, the time stepping procedure is expensive in storage and has stability problems for badly chosen time step sizes. The first problem can be overcome by using the Convolution Quadrature Method (CQM) for time discretisation. This as well improves the stability. However, still the storage requirements are large.
A recently published reformulation of the CQM by Banjai and Sauter [Rapid solution of the wave equation in unbounded domains, SIAM J. Numer. Anal., 47, 227–249] reduces the time stepping procedure to the solution of decoupled problems in Laplace domain. This new version of the CQM is applied here to elastodynamics. The storage is reduced to nearly the amount necessary for one calculation in Laplace domain. The properties of the original method concerning stability in time are preserved. Further, the only parameter to be adjusted is still the time step size. The drawback is that the time history of the given boundary data has to be known in advance. These conclusions are validated by the examples of an elastodynamic column and a poroelastodynamic half space.

1 Introduction

The Boundary Element Method (BEM) in time domain is especially import to treat wave propagation problems in infinite and semi-infinite domains. In this application the main advantage of this method becomes obvious, i.e., its ability to model the Sommerfeld radiation condition correctly. Certainly this is not the only advantage of a time domain BEM but very often the main motivation as, e.g., in earthquake engineering.

The first boundary integral formulation for elastodynamics was published by Cruse and Rizzo [9]. This formulation performs in Laplace domain with a subsequent inverse transformation to time domain to achieve results for the transient behavior. The corresponding formulation in Fourier domain, i.e., frequency domain, was presented by Domínguez [11]. The first boundary element formulation directly in the time domain was developed by Mansur for the scalar wave equation and for elastodynamics with zero initial conditions [27]. The extension of this formulation to non-zero initial conditions was presented by Antes [4]. Detailed information about this procedure may be found in the book of Domínguez [10]. A comparative study of these possibilities to treat elastodynamic problems with BEM was given by Manolis [26]. A completely different approach to handle dynamic problems utilizing static fundamental solutions is the so-called dual reciprocity BEM. This method was introduced by Nardini and Brebbia [30] and details may be found in the monograph of Partridge et al. [31]. A very detailed review on elastodynamic boundary element formulations and a list of applications can be found in two articles of Beskos [7, 8].

The above listed methodologies to treat elastodynamic problems with the BEM show mainly the two ways: direct in time domain or via an inverse transformation in Laplace domain. Mostly, the latter is used, e.g., Ahmad and Manolis [3]. Since all numerical inversion formulas depend on a proper choice of their parameters [29], a direct evaluation in time domain seems to be preferable. Also, it is more natural to work in the real time domain and observe the phenomenon as it evolves. But, as all time-stepping procedures, such a formulation requires an adequate choice of the time step size. An improper chosen time step size leads to instabilities or numerical damping. Four procedures to improve the stability of the classical dynamic time-stepping BE formulation can be quoted: the first employs modified numerical time marching procedures, e.g., [5] for acoustics, [32] for elastodynamics; the second employs a modified fundamental solution, e.g., [33] for elastodynamics; the third employs an additional integral equation for velocities [28]; and the last uses weighting methods, e.g., [42] for elastodynamics and [43] for acoustics.

Beside these improved approaches there exist the possibility to solve the convolution integral in the boundary integral equation with the so-called Convolution Quadrature Method (CQM) proposed by Lubich [21, 22]. Applications to hyperbolic and parabolic integral equations can be found in [25, 24]. The CQM utilizes the Laplace domain fundamental solution and results not only in a more stable time stepping procedure but also damping effects in case of visco- or poroelasticity can be taken into account (see [37, 38, 34]). The motivation to use the CQM in these engineering applications is that only the Laplace domain fundamental solutions are required. This fact is also used for BE formulations in cracked anisotropic elastic [44] or piezoelectric materials [13]. Another aspect is the better stability behavior compared with the above mentioned formulation. For acoustics this may be found in [1, 2] and in elastodynamics in [35].

In the framework of fast BE formulations the CQM is used in a Panel-clustering formulation for the Helmholtz equation by Hackbusch et al. [17]. Recently, some newer mathematical aspects of the CQM have been published by Lubich [23].

Important for the paper at hand, an essential reformulation of the CQM in case of integral equations has been published by Banjai and Sauter [6]. The proposed formulation transfers the time stepping procedure to the solution of decoupled Laplace domain problems. The main parameter of the method is still the applied time step size. In this paper, some stability proofs with respect to the time dependent behavior can be found. Here, this technique is applied to elastodynamics for a collocation and a symmetric Galerkin formulation. At the end some numerical studies are performed concerning the sensitivity on the mesh size, the time step size, and on the precision of the equation solver. To show the applicability of the reformulated CQM to inelastic BE formulations the displacement results for wave propagation in a poroelastic half space are presented.

Throughout this paper, vectors and tensors are denoted by bold symbols and matrices by sans serif and upright symbols. The Laplace transform of a function $f(t)$ is denoted by $\hat{f}(s)$ with the complex Laplace parameter s.

2 Boundary integral equation

The hyperbolic partial differential equation to be considered in this work is the elastodynamic system, which describes the displacement field $\mathbf{u}(\mathbf{x},t)$ of an elastic solid under the assumptions of linear elasticity. Describing with $\mathbf{x}$ and t the position in the three-dimensional Euclidean space $\mathbb{R}^3$ and the time point from the interval $(0,\infty)$ the hyperbolic initial boundary value problem is

$$\begin{aligned} c_1^2\nabla(\nabla\cdot\mathbf{u}(\mathbf{x},t)) - c_2^2\nabla\times(\nabla\times\mathbf{u}(\mathbf{x},t)) &= \frac{\partial^2\mathbf{u}}{\partial t^2}(\mathbf{x},t) \quad (\mathbf{x},t)\in\Omega\times(0,\infty) \\ \mathbf{u}(\mathbf{y},t) &= \mathbf{g}_D(\mathbf{y},t) \quad (\mathbf{y},t)\in\Gamma_D\times(0,\infty) \\ \mathbf{t}(\mathbf{y},t) &= \mathbf{g}_N(\mathbf{y},t) \quad (\mathbf{y},t)\in\Gamma_N\times(0,\infty) \\ \mathbf{u}(\mathbf{x},0) = \frac{\partial\mathbf{u}}{\partial t}(\mathbf{x},0) &= \mathbf{0} \quad (\mathbf{x},t)\in\Omega\times(0)\,. \end{aligned} \tag{1}$$

The material properties of the solid are represented by the wave speeds

$$c_1 = \sqrt{\frac{E\,(1-\nu)}{\rho\,(1-2\nu)\,(1+\nu)}} \qquad c_2 = \sqrt{\frac{E}{\rho 2\,(1+\nu)}}\,, \tag{2}$$

with the material data Young's modulus E, Poisson's ration ν, and the mass density ρ. The first statement in (1) requires the fulfillment of the partial differential equation in the spatial domain Ω for all times $0<t<\infty$. This spatial domain Ω has the boundary Γ which is subdivided into two disjoint sets Γ_D and Γ_N at which boundary conditions are prescribed. The Dirichlet boundary condition is the second statement of (1) and assigns a given datum $\mathbf{g}_D$ to the displacement $\mathbf{u}$ on the part Γ_D of the boundary. Similarly, the Neumann boundary condition is the third statement in which the datum $\mathbf{g}_N$ is assigned to the surface traction $\mathbf{t}$, which is defined by

$$\mathbf{t}(\mathbf{y},t) = (\mathcal{T}\mathbf{u})(\mathbf{y},t) = \lim_{\Omega\ni\mathbf{x}\to\mathbf{y}\in\Gamma}[\sigma(\mathbf{x},t)\cdot\mathbf{n}(\mathbf{y})]\,. \tag{3}$$

In (3), σ is the stress tensor depending on the displacement field $\mathbf{u}$ according to the strain-displacement relationship and Hooke's law. For later purposes the traction operator $\mathcal{T}$ is defined, which maps the displacement field $\mathbf{u}$ to the surface traction $\mathbf{t}$. The boundary conditions have to hold for all times and may be also prescribed in each direction by different types, e.g., roller bearings. Finally, in the last statement of (1) the condition of a quiescent past is given which implies homogeneous initial conditions.

The representation formula may be derived from the dynamic reciprocal identity [41] or also from a weighted residual statement. With the Riemann convolution defined as

$$(g*h)(\mathbf{x},t) = \int_0^t g(\mathbf{x},t-\tau)h(\tau)\,\mathrm{d}\tau, \tag{4}$$

and the fundamental solution $\mathbf{U}(\mathbf{x}-\mathbf{y},t-\tau)$ of equation (1) the representation formula

$$\mathbf{u}(\mathbf{x},t) = \int_0^t \int_\Gamma \mathbf{U}(\mathbf{x}-\mathbf{y},t-\tau)\mathbf{t}(\mathbf{y},\tau)\,\mathrm{d}s_\mathbf{y}\,\mathrm{d}\tau - \int_0^t \int_\Gamma (\mathcal{T}_\mathbf{y}\mathbf{U})(\mathbf{x}-\mathbf{y},t-\tau)\mathbf{u}(\mathbf{y},\tau)\,\mathrm{d}s_\mathbf{y}\,\mathrm{d}\tau \qquad \mathbf{x}\in\Omega, \mathbf{y}\in\Gamma \tag{5}$$

is given. Here, the surface measure $\mathrm{d}s_\mathbf{y}$ carries its subscript in order to emphasize that the integration variable is $\mathbf{y}$. Similarly, $\mathcal{T}_\mathbf{y}$ indicates that the derivatives involved in the computation of the surface traction due to equation (3) are taken with respect to the variable $\mathbf{y}$. Explicit expressions for the used fundamental solutions can be found, for instance, in [18]. By means of equation (5), the unknown $\mathbf{u}$ is given at any point $\mathbf{x}$ inside the domain Ω and at any time $0<t<\infty$, if the boundary data $\mathbf{u}(\mathbf{y},\tau)$ and $\mathbf{t}(\mathbf{y},\tau)$ are known for all points $\mathbf{y}$ of the boundary Γ and times $0<\tau<t$.

The first boundary integral equation is obtained by taking expression (5) to the boundary. Using operator notation, this boundary integral equation reads

$$(\mathcal{V}*\mathbf{t})(\mathbf{x},t) = \mathcal{C}(\mathbf{x})\mathbf{u}(\mathbf{x},t) + (\mathcal{K}*\mathbf{u})(\mathbf{x},t) \qquad (\mathbf{x},t)\in\Gamma\times(0,\infty)\,. \tag{6}$$

The introduced operators are the single layer operator $\mathcal{V}$, the integral-free term $\mathcal{C}$, and the double layer operator $\mathcal{K}$ which are defined as

$$(\mathcal{V}*\mathbf{t})(\mathbf{x},t) = \int_0^t \int_\Gamma \mathbf{U}(\mathbf{x}-\mathbf{y},t-\tau)\mathbf{t}(\mathbf{y},\tau)\,\mathrm{d}s_\mathbf{y}\,\mathrm{d}\tau \tag{7a}$$

$$\mathcal{C}(\mathbf{x}) = \mathcal{I} + \lim_{\varepsilon\to 0} \int_{\partial B_\varepsilon(\mathbf{x})\cap\Omega} (\mathcal{T}_\mathbf{y}\mathbf{U})^\top(\mathbf{x}-\mathbf{y},0)\,\mathrm{d}s_\mathbf{y} \tag{7b}$$

$$(\mathcal{K}*\mathbf{u})(\mathbf{x},t) = \lim_{\varepsilon\to 0} \int_0^t \int_{\Gamma\setminus B_\varepsilon(\mathbf{x})} (\mathcal{T}_\mathbf{y}\mathbf{U})^\top(\mathbf{x}-\mathbf{y},t-\tau)\mathbf{u}(\mathbf{y},\tau)\,\mathrm{d}s_\mathbf{y}\,\mathrm{d}\tau\,. \tag{7c}$$

In these expressions, $B_\varepsilon(\mathbf{x})$ denotes a ball of radius ε centered at $\mathbf{x}$ and $\partial B_\varepsilon(\mathbf{x})$ is its surface. Note that the single layer operator (7a) involves a weakly singular integral and the double layer operator (7c) has to be understood in the sense of a principal value.

Application of the traction operator $\mathcal{T}_x$ to the dynamic representation formula (5) yields the second boundary integral equation

$$(\mathcal{D} * \mathbf{u})(\mathbf{x},t) = (\mathcal{I} - \mathcal{C}(\mathbf{x}))\,\mathbf{t}(\mathbf{x},t) - (\mathcal{K}' * \mathbf{t})(\mathbf{x},t) \qquad \mathbf{x} \in \Gamma\,. \tag{8}$$

The newly introduced operators are the adjoint double layer operator $\mathcal{K}'$ and the hyper-singular operator $\mathcal{D}$. They are defined as

$$(\mathcal{K}' * \mathbf{t})(\mathbf{x},t) = \lim_{\varepsilon\to 0} \int_0^t \int_{\Gamma\setminus B_\varepsilon(\mathbf{x})} (\mathcal{T}_{\mathbf{x}}\mathbf{U})(\mathbf{x}-\mathbf{y},t-\tau)\mathbf{t}(\mathbf{y},\tau)\,\mathrm{d}s_{\mathbf{y}}\,\mathrm{d}\tau \tag{9a}$$

$$(\mathcal{D} * \mathbf{u})(\mathbf{x},t) = -\lim_{\varepsilon\to 0} \int_0^t \mathcal{T}_{\mathbf{x}} \int_{\Gamma\setminus B_\varepsilon(\mathbf{x})} (\mathcal{T}_{\mathbf{y}}\mathbf{U})^\top(\mathbf{x}-\mathbf{y},t-\tau)\mathbf{u}(\mathbf{y},\tau)\,\mathrm{d}s_{\mathbf{y}}\,\mathrm{d}\tau\,. \tag{9b}$$

The hyper-singular operator has to be understood in the sense of a finite part.

For the solution of mixed initial boundary value problems of the form (1), a non-symmetric formulation by means of the first boundary integral equation (6) in combination with a collocation technique will be used. A symmetric formulation is obtained using both the first and the second boundary integral equation, (6) and (8).

Symmetric formulation First, the Dirichlet datum $\mathbf{u}$ and the Neumann datum $\mathbf{t}$ are decomposed into

$$\mathbf{u} = \tilde{\mathbf{u}} + \tilde{\mathbf{g}}_D \qquad \text{and} \qquad \mathbf{t} = \tilde{\mathbf{t}} + \tilde{\mathbf{g}}_N\,, \tag{10}$$

with arbitrary but fixed extensions, $\tilde{\mathbf{g}}_D$ and $\tilde{\mathbf{g}}_N$, of the given Dirichlet and Neumann data, $\mathbf{g}_D$ and $\mathbf{g}_N$. They are introduced such that

$$\begin{aligned} \tilde{\mathbf{g}}_D(\mathbf{x},t) &= \mathbf{g}_D(\mathbf{x},t)\,, \qquad (\mathbf{x},t) \in \Gamma_D \times (0,\infty) \\ \tilde{\mathbf{g}}_N(\mathbf{x},t) &= \mathbf{g}_N(\mathbf{x},t)\,, \qquad (\mathbf{x},t) \in \Gamma_N \times (0,\infty) \end{aligned} \tag{11}$$

holds. The extension $\tilde{\mathbf{g}}_D$ of the given Dirichlet datum has to be continuous due to regularity requirements [40].

In order to establish a symmetric formulation, the first boundary integral equation (6) is used only on the Dirichlet boundary Γ_D whereas the second one (8) is used only on the Neumann part Γ_N. Taking the prescribed boundary conditions (1) into account and inserting the decompositions (10) into both integral equations leads to the symmetric formulation for the unknowns $\tilde{\mathbf{u}}$ and $\tilde{\mathbf{t}}$

$$\begin{aligned} \mathcal{V} * \tilde{\mathbf{t}} - \mathcal{K} * \tilde{\mathbf{u}} &= \mathbf{f}_D, \quad (\mathbf{x},t) \in \Gamma_D \times (0,\infty) \\ \mathcal{D} * \tilde{\mathbf{u}} + \mathcal{K}' * \tilde{\mathbf{t}} &= \mathbf{f}_N, \quad (\mathbf{x},t) \in \Gamma_N \times (0,\infty) \end{aligned} \tag{12}$$

with the abbreviations

$$\begin{aligned} \mathbf{f}_D &= \mathcal{C}\tilde{\mathbf{g}}_D + \mathcal{K} * \tilde{\mathbf{g}}_D - \mathcal{V} * \tilde{\mathbf{g}}_N \\ \mathbf{f}_N &= (\mathcal{I} - \mathcal{C})\,\tilde{\mathbf{g}}_N - \mathcal{K}' * \tilde{\mathbf{g}}_N - \mathcal{D} * \tilde{\mathbf{g}}_D\,. \end{aligned} \tag{13}$$

3 Boundary element formulation

A boundary element formulation is derived following the usual procedure.

3.1 Semi-discrete equations

Let the boundary Γ of the considered domain be represented in the computation by an approximation Γ_h which is the union of geometrical elements

$$\Gamma_h = \bigcup_{e=1}^{N_e} \tau_e \,. \tag{14}$$

τ_e denote boundary elements, e.g., surface triangles as in this work, and their total number is N_e. Now, the boundary functions $\tilde{\mathbf{u}}$ and $\tilde{\mathbf{t}}$ are approximated with shape functions φ_i or ψ_j, which are defined with respect to the geometry partitioning (14), and time dependent coefficients u_k^i and t_k^j. This yields for the k-th component of the data

$$u_k(\mathbf{y},t) = \sum_{i=1}^{N} u_k^i(t)\varphi_i(\mathbf{y}) \qquad \text{and} \qquad t_k(\mathbf{y},t) = \sum_{j=1}^{M} t_k^j(t)\psi_j(\mathbf{y}) \,. \tag{15}$$

Inserting these spatial shape functions in the boundary integral equations (12) and (6), respectively, and applying on the first a Galerkin scheme and on the latter a collocation method, results in the two semi-discrete equation systems. The Galerkin method with (12) yields

$$\begin{bmatrix} \mathsf{V} & -\mathsf{K} \\ \mathsf{K}^\mathsf{T} & \mathsf{D} \end{bmatrix} * \begin{bmatrix} \mathsf{t} \\ \mathsf{u} \end{bmatrix} = \begin{bmatrix} \mathsf{f}_D \\ \mathsf{f}_N \end{bmatrix} \tag{16}$$

and the collocation method yields for the first integral equation (6)

$$\mathsf{V} * \mathsf{t} = \mathsf{C}\mathsf{u} + \mathsf{K} * \mathsf{u} \,. \tag{17}$$

In the equations (16) and (17), the time is still continuous and the convolution has to be performed. Further, the notation of matrices/vectors with sans serif letters denotes that in these matrices the data at all nodes and all degrees of freedom are collected.

3.2 Convolution Quadrature Method

Next, the temporal discretization by the CQM has to be introduced. Its basic idea is to approximate the convolution integral (4) by a quadrature formula on an equidistant time grid of step size Δt, i.e., $0 = t_0 < \Delta t = t_1 < \cdots < n\Delta t = t_n$,

$$(g * h)(\mathbf{x}, t_n) \approx \sum_{k=0}^{n} \omega_{n-k}(\Delta t, \gamma, \hat{g}) f(k\Delta t) \,. \tag{18}$$

In this expression, the quadrature weights ω_{n-k} depend on the step size Δt, the quotient of the characteristic polynomials γ of the underlying A-stable multistep method, and the Laplace

transformed function $\hat{g}$. The quadrature weights are computed following

$$\omega_{n-k}(\Delta t,\gamma,\hat{g}) = \frac{\mathscr{R}^{-(n-k)}}{L}\sum_{\ell=0}^{L-1}\hat{g}\left(s_\ell\right)\zeta^{-(n-k)\ell} \qquad \zeta = e^{\frac{2\pi \mathrm{i}}{L}}$$
$$\text{with the complex 'frequency'} \qquad s_\ell = \frac{\gamma\left(\zeta^\ell \mathscr{R}\right)}{\Delta t}\ . \tag{19}$$

Confer [35] for the technical details on the computation of these quadrature weights ω_{n-k}. The notation *complex frequency* expresses that these complex numbers at which the quadrature weights are evaluated may be interpreted as a computation at distinct frequencies. However, these points are complex valued.

Inserting the CQM in the semi-discrete integral equation, e.g., in (17), yields an equation system for $n = 0,1,\ldots,N-1$

$$\sum_{k=0}^{n}\frac{\mathscr{R}^{-(n-k)}}{L}\sum_{\ell=0}^{L-1}\left[\hat{\mathsf{V}}\left(s_\ell\right)\mathsf{t}\left(k\Delta t\right)-\hat{\mathsf{K}}\left(s_\ell\right)\mathsf{u}\left(k\Delta t\right)\right]\zeta^{-(n-k)\ell} = \mathsf{C}\mathsf{u}\left(n\Delta t\right)\ , \tag{20}$$

where N denotes the total amount of time steps. Note that in these equations the boundary data are still in time domain whereas the matrices with the fundamental solutions are evaluated in Laplace domain. Nevertheless, it is still a time stepping procedure.

In [35], it is shown that for an efficient solution the value of L should be chosen $L = N$. Further, it should be remembered that the quadrature weights ω_n are set to zero for negative indices, i.e., in the framework of BEM the causality is ensured. This can be used such that the sum over k can be extended to $N-1$. The two sums in (20) are exchanged. Further, $\mathscr{R}$ as well as ζ have the exponent $n-k$ and are splitted in two expressions with the exponents k and n separately. These operations yield

$$\frac{\mathscr{R}^{-n}}{N}\sum_{\ell=0}^{N-1}\left[\hat{\mathsf{V}}\left(s_\ell\right)\sum_{k=0}^{N-1}\mathscr{R}^k\mathsf{t}\left(k\Delta t\right)\zeta^{k\ell}-\hat{\mathsf{K}}\left(s_\ell\right)\sum_{k=0}^{N-1}\mathscr{R}^k\mathsf{u}\left(k\Delta t\right)\zeta^{k\ell}\right]\zeta^{-n\ell} = \mathsf{C}\mathsf{u}\left(n\Delta t\right)\ . \tag{21}$$

Both inner sums can be seen as a weighted FFT of the time dependent nodal values. These expression will be abbreviated with

$$\mathsf{u}_\ell^* = \sum_{k=0}^{N-1}\mathscr{R}^k\mathsf{u}\left(k\Delta t\right)\zeta^{k\ell} \qquad \mathsf{t}_\ell^* = \sum_{k=0}^{N-1}\mathscr{R}^k\mathsf{t}\left(k\Delta t\right)\zeta^{k\ell}\ , \tag{22}$$

where the respective inverse operation is

$$\mathsf{u}\left(n\Delta t\right) = \frac{\mathscr{R}^{-n}}{N}\sum_{k=0}^{N-1}\mathsf{u}_\ell^*\zeta^{-n\ell} \qquad \mathsf{t}\left(n\Delta t\right) = \frac{\mathscr{R}^{-n}}{N}\sum_{k=0}^{N-1}\mathsf{t}_\ell^*\zeta^{-n\ell}\ . \tag{23}$$

With this in mind the hyperbolic integral equation (17) is reduced to the solution of N elliptic problems for the complex 'frequency' $s_\ell, \ell = 0,1,\ldots,N-1$

$$\hat{\mathsf{V}}\left(s_\ell\right)\mathsf{t}_\ell^* - \hat{\mathsf{K}}\left(s_\ell\right)\mathsf{u}_\ell^* = \mathsf{C}\mathsf{u}_\ell^*\ . \tag{24}$$

Applying the same operations as above on the Galerkin scheme (16) the decoupled Laplace domain problems

$$\begin{bmatrix} \hat{\mathsf{V}} & -\hat{\mathsf{K}} \\ \hat{\mathsf{K}}^{\mathsf{T}} & \hat{\mathsf{D}} \end{bmatrix} (s_\ell) \begin{bmatrix} \mathsf{t}^*_\ell \\ \mathsf{u}^*_\ell \end{bmatrix} = \begin{bmatrix} \mathsf{f}^*_{D\ell} \\ \mathsf{f}^*_{N\ell} \end{bmatrix} \tag{25}$$

are obtained. The right hand side in (25) is from the same structure

$$\begin{aligned} \mathsf{f}^*_{D\ell} &= \left(\mathsf{C} + \hat{\mathsf{K}}(s_\ell)\right) \mathsf{g}^*_{D\ell} - \hat{\mathsf{V}}(s_\ell)\, \mathsf{g}^*_{N\ell} \\ \mathsf{f}^*_{N\ell} &= \left(\mathsf{I} - \mathsf{C} - \hat{\mathsf{K}}'(s_\ell)\right) \mathsf{g}^*_{N\ell} - \hat{\mathsf{D}}(s_\ell)\, \mathsf{g}^*_{D\ell}\,, \end{aligned} \tag{26}$$

where $\mathsf{g}^*_{D\ell}$ and $\mathsf{g}^*_{N\ell}$ denote the transformed given boundary data corresponding to the ℓ-th complex frequency. The transformation is performed similar to (22). With these operations the time stepping procedure is reduced to the solution of decoupled Laplace domain problems.

Looking closely on the expression ζ in (19) makes it obvious that the equations (22) and (23) can be computed fast with the technique known from the FFT. Further, due to the structure of s_ℓ in (19) only $N/2$ problems have to be solved because the other half is determined as the complex conjugate solution. Finally, the time dependent response is achieved with (23).

Remark 1: Certainly, the above presented reformulation of the CQM based on the paper by Banjai and Sauter [6] can be applied to any other CQM based BE formulation. In the following example section, a poroelastodynamic half space will be calculated with this technique. Details of the poroelastodynamic formulation can be found in [36].

Remark 2: This reformulation of the CQM may be seen as a calculation in Laplace domain with an inverse back transformation. However, compared to the known techniques with the problem of finding adequate parameters for the inverse transformation or an adequate numerical technique at all (see, e.g., [29, 14]) in the above formulation only the time step size (a physical quantity) has to be determined. The following numerical tests will show that this physical parameter can be determined as in the time stepping procedure (20), i.e., it is selected with relation to the element size and the wave speed.

3.3 Numerical solution

The remaining part is the numerical realisation of the above given procedure. All regular integrals are performed with Gaussian quadrature formulas. The singular integrals can be performed with known techniques from elliptic problems. In the following, for the symmetric Galerkin formulation the regularisation based on partial integration as presented by Kielhorn and Schanz [19] is applied. The resulting weakly singular integrals are solved with the formulas by Erichsen and Sauter [12]. In the collocation technique the strong singular integrals are performed with the method from Guiggiani and Gigante [16] and the weak singular ones with polar coordinate transformation. Finally, the equation systems for the collocation method (24) are treated with a LU-decomposition. For the Galerkin scheme (25) the *Schur-Complement-System* is computed by

$$\hat{\mathsf{S}} = \hat{\mathsf{K}}^{\mathsf{T}} \hat{\mathsf{V}}^{-1} \hat{\mathsf{K}} + \hat{\mathsf{D}}\,. \tag{27}$$

Due to the symmetry and the positive definiteness of $\hat{\mathsf{V}}$ and $\hat{\mathsf{D}}$ the Schur-Complement $\hat{\mathsf{S}}$ is also symmetric and positive definite. For the solution an iterative GMRES-solver is used. Hence, the

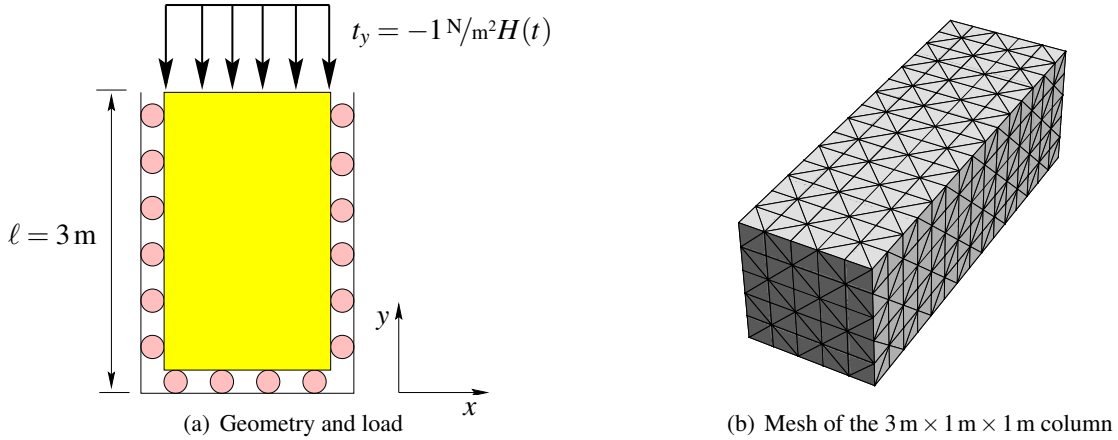

(a) Geometry and load

(b) Mesh of the $3\,\mathrm{m} \times 1\,\mathrm{m} \times 1\,\mathrm{m}$ column

Figure 1: Geometry, loading, and the mesh of the column

displacement field u^*_ℓ and the tractions t^*_ℓ can be found by solving

$$\hat{\mathsf{S}}\mathsf{u}^*_\ell = \mathsf{f}^*_{N\ell} - \hat{\mathsf{K}}^\mathsf{T}\hat{\mathsf{V}}^{-1}\mathsf{f}^*_{D\ell} \tag{28}$$

and

$$\mathsf{t}^*_\ell = \hat{\mathsf{V}}^{-1}\left(\mathsf{f}^*_{D\ell} + \hat{\mathsf{K}}\mathsf{u}^*_\ell\right) \tag{29}$$

for every complex frequency s_ℓ, $\ell = 0, \ldots, N/2$.

4 Numerical examples

In this section, the numerical behavior of this reformulated CQM in the application on an elastodynamic column is studied. Further, results for wave propagation phenomena in a poroelastic half space are presented. For all computations a Backward Difference Formula of second order (BDF2) as multistep method is used. The parameter $\mathscr{R}$ can be adjusted as in the original formulation to $\mathscr{R}^N = \sqrt{\varepsilon}$ with $10^{-10} < \varepsilon < 10^{-3}$ which may vary between different physical problem types and between 2-d and 3-d. However, it is independent of the geometry and boundary conditions.

4.1 Elastic column

A one dimensional (1-d) column of length 3 m as sketched in Fig. 1(a) is considered. It is assumed that the side walls and the bottom are rigid and frictionless. Hence, the displacements normal to the surface are blocked and the column is otherwise free to slide only parallel to the wall. At the top, the stress vector $t_y = -1\,\mathrm{N/m^2} H(t)$ is given. Due to these restrictions, the 3-d continuum is reduced to a 1-d column with the only degree of freedom in y-direction. This 1-d column has been solved analytically in [15] and its result is compared to the boundary element solution for a 3-d rod ($3\,\mathrm{m} \times 1\,\mathrm{m} \times 1\,\mathrm{m}$). The used BE formulation is the symmetric Galerkin scheme sketched before, where the traction field is approximated on linear triangles

Table 1: Material data for the elastic column and the poroelastic half space

	E $\mathrm{N/m^2}$	ν -	ρ $\mathrm{kg/m^3}$	ϕ -	R $\mathrm{N/m^2}$	ρ_f $\mathrm{kg/m^3}$	α -	κ $\mathrm{m^4/Ns}$
	elastic column							
steel	$2.11 \cdot 10^{11}$	0	7850					
	poroelastic half space							
soil	$2.544 \cdot 10^{8}$	0.298	1884	0.48	$1.2 \cdot 10^{9}$	1000	0.981	$3.55 \cdot 10^{-9}$

with constant shape functions and the displacement field with linear ones. Material data used are those of steel modified with Poisson's ratio set to zero (see Tab. 1).

The meshes used in the following are four different ones which are basically a refinement or coarsening of that shown in Fig. 1(b). They will be denoted

- mesh 1: uniform with 112 elements on 58 nodes
- mesh 2: uniform with 448 elements on 226 nodes
- mesh 3: uniform with 700 elements on 352 nodes as displayed in Fig. 1(b)
- mesh 4: uniform with 2800 elements on 1402 nodes.

In Fig. 2, the displacement results versus time at the free end are plotted for the meshes 1,2, and 3. The time step size for all three calculations are adjusted to $\beta = 0.3$. This dimensionless value used for the comparison is $\beta = {c_1 \Delta t}/{r_e}$, with the characteristic length of the elements r_e. Here, the cathethus of the triangles is used. The differences for the displacements in Fig. 2 are not too large. In the second half of the figure, the tractions at the bottom of the column show differences. The coarsest mesh 1 yields not satisfactory results for larger times. The overshooting following the jumps in the solution are unavoidable but a refined mesh reduces the duration of this disturbance. It is exactly the same behavior as in the 'old' CQM based BEM as presented, e.g., in [19]. That is why no comparison between the old formulation and the reformulated version is given. They can not be distinguished in a plot.

In Fig. 3, the displacement at the top and the traction at the bottom are plotted versus time for different time step sizes. These are expressed with β to have a better comparison. The results are computed with mesh 2. The instability for the smallest value $\beta = 0.1$ is clearly observed in the traction solution. The other extreme value, $\beta = 0.7$, shows some numerical damping and not the best results for the traction. All other results are acceptable, where as in the original formulation a value $\beta = 0.2$ yields the best results. Hence, also the sensitivity on the choice of the time step size is the same as in the original formulation. A time step size in the range $0.1 < \beta < 0.5$ may be recommended.

It must be remarked that here the main advantage of the presented formulation compared to usual computations in Laplace or Fourier domain can be observed. The parameter responsible for the quality of the results is the time step size and not any sophisticated parameter of the

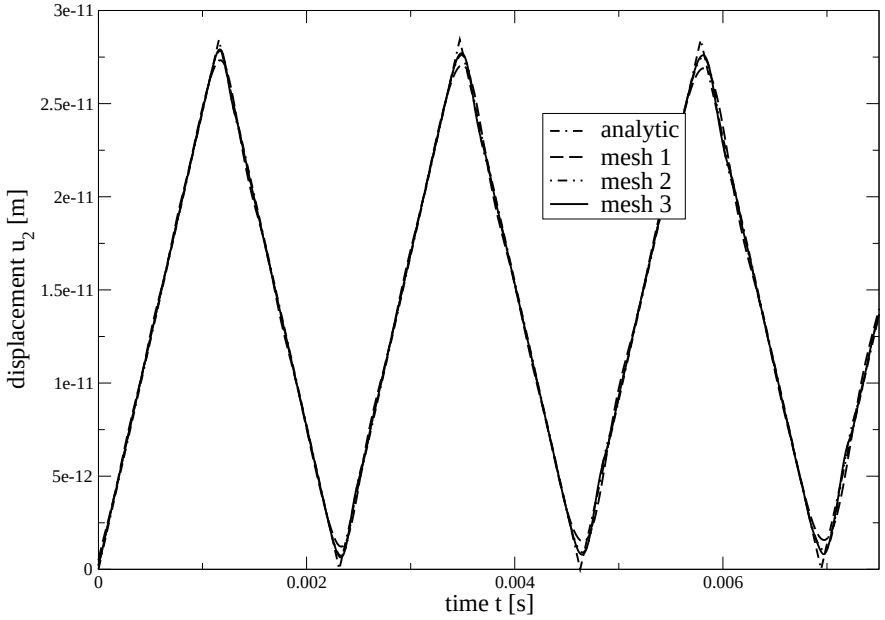

(a) Displacement at the top

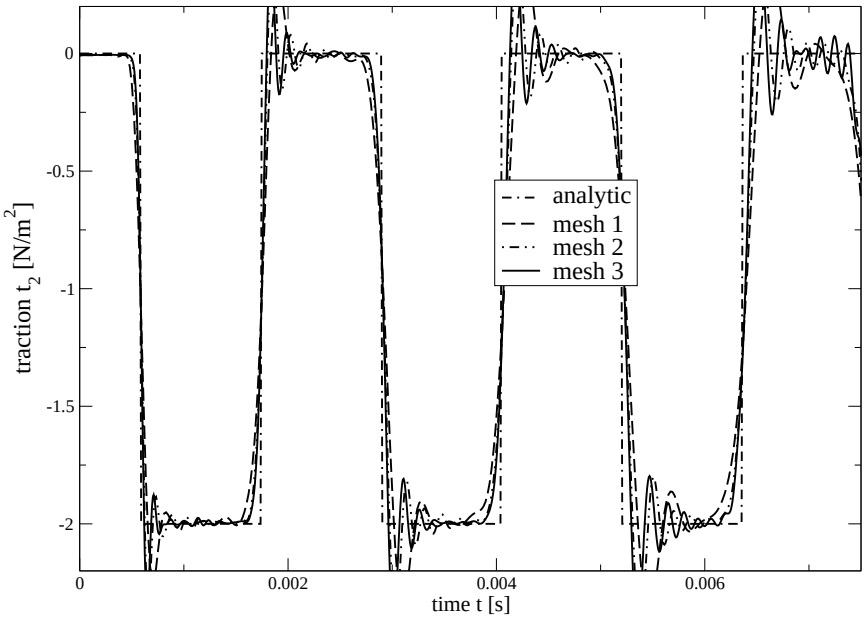

(b) Traction at the bottom

Figure 2: Displacement and traction versus time for different meshes compared with the analytical solution

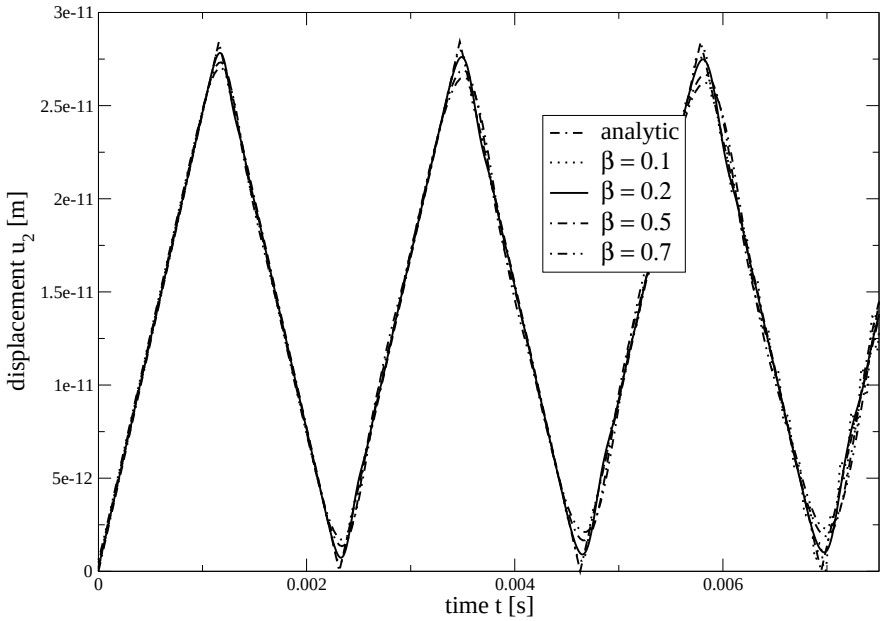

(a) Displacement at the top

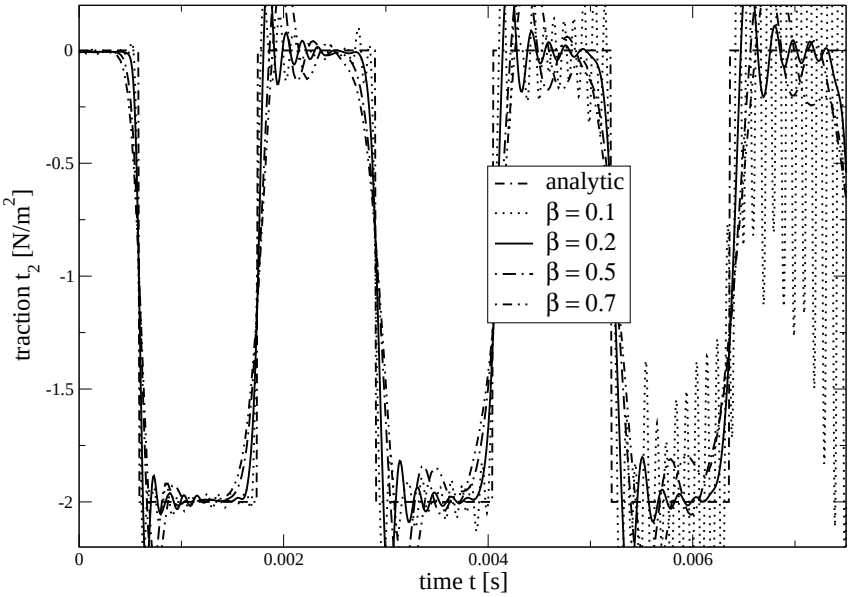

(b) Traction at the bottom

Figure 3: Displacement and traction versus time for different time step sizes, i.e., β values, compared with the analytical solution

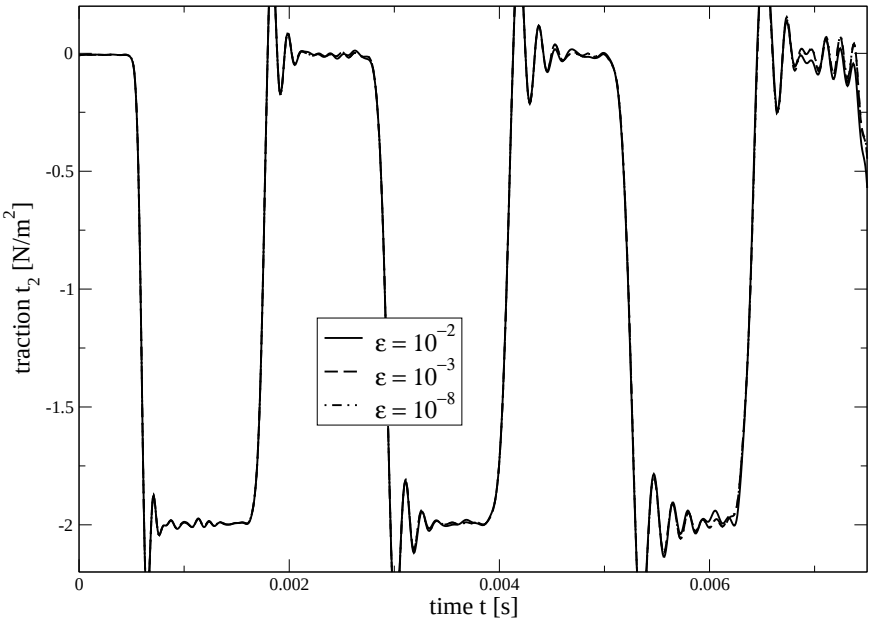

Figure 4: Traction versus time for different precisions ε of the iterative solver

various numerical inverse transformation algorithms. This value is oriented on the physics of the problem, i.e., it must be adjusted to the wave speed in relation to the mesh size.

The next parametric study concerns the solution of the equation system. For larger problems iterative solvers may be used. Hence, the question arise what is the influence of the solver precision on the time dependent results. Here, a GMRES is used. In Fig. 4, the traction solutions for mesh 4 are plotted calculated with different precisions of the GMRES. The displacement solutions are not displayed because no differences would be visible. In the traction solution, only for the coarse value of $\varepsilon = 10^{-2}$ negative effects for large times may be observed. It may be concluded that the solver precision is not so important. But, it must be remarked that the solver works in Laplace domain and, hence, eigenfrequencies even if they are damped may cause problems. Further, it is recommended to think on proper preconditioners. Last, it should be mentioned that this ε has nothing to do with the ε to determine $\mathscr{R}$ as discussed at the begining of this section.

4.2 Poroelastic half space

The second example is a poroelastic half space modelled with Biot's theory. The collocation BE formulation proposed in [35] with the new formulation of the CQM is applied. To be able to solve the equation system dimensionless variables are introduced as suggested in [39]. Details of the poroelastic BE formulation based on the reformulation of the CQM and numerical studies on the sensitivity with respect to the time step size can be found in [36]. These tests confirm the observation in the paragraph above, the new formulation behaves like the old one.

The following results are obtained with linear shape functions for all unknowns, i.e., the solid

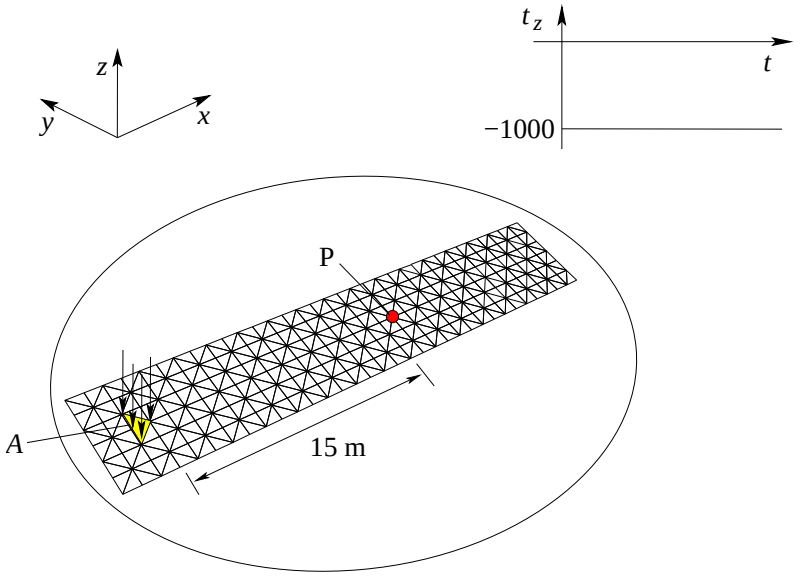

Figure 5: Poroelastic half space: Mesh and the time dependence of the load

displacements, the pore pressure, the tractions, and the flux. The geometry is approximated by linear triangles as sketched in Fig. 5. The half space is loaded in area A by a total stress vector $t_z = -1000\,\mathrm{N/m^2} H(t)$ kept constant from $t = 0\,\mathrm{s}$ on. The material data are those of a water saturated soil taken from literature [20] and listed in Tab. 1. There, ϕ, R, ρ_f, α, and κ denote the porosity, Biot's constant, density of the fluid, Biot's stress coefficient, and the permeability, respectively.

In Fig. 6, the vertical solid displacement u_z is plotted versus time for the point P in 15 m distance to the load. The poroelastic result is compared to two elastodynamic solutions denoted by 'drained' and 'undrained'. This means the shear modulus is the same as in the poroelastic case but in the drained case the same Poisson's ratio is used whereas in the undrained case the undrained Poisson's ratio is inserted. Additionally, a calculation with the 'old' CQM based BE formulation is presented, lying over the 'new' CQM based formulation.

The arrival time of the compression wave $t \approx 0.014\,\mathrm{s}$ and the Rayleigh pole are clearly observed. Further, as expected, the poroelastic solution is between the two extreme elastodynamic cases, whereas in the early time it follows the undrained behavior and later (in the second half of the picture) it approaches the drained solution. The solution denoted 'long time' is obtained with a very large time step size to reach such long observation times. That is the reason why this solution in the short time range does not resolve the arrival of the waves correctly.

5 Conclusion

A reformulated version of the Convolution Quadrature Method (CQM) has been applied to the elastodynamic boundary integral equation in time domain. Both, a symmetric Galerkin method and a collocation method has been presented. Clearly, this reformulation of the CQM can be

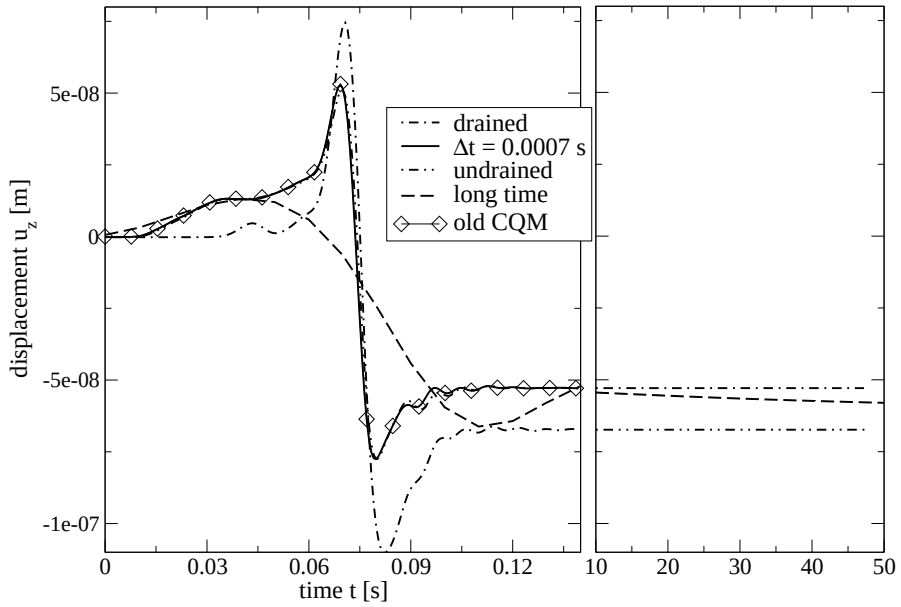

Figure 6: Vertical displacement at point P: Short and long time behavior

applied to any other application in time domain BE formulations. Here, additionally to the elastodynamic example a poroelastodynamic example has been shown. Overall, the presented methodology reduces the storage requirement to the size of one complex valued system matrix and shows the same sensitivity on the time step size as the older formulation presented by Schanz [35]. The price to be payed for this reduction in storage is that in each step the system of equations has to be solved. But, for future work, this reformulated CQM allows the application of fast BE techniques which are mostly known for elliptic problems and not for hyperbolic ones.

In some sense this reformulation is similar to classical formulations in Laplace or Fourier domain with numerical inverse transformations. It shares the disadvantage that the time history of the given boundary data has to be known in advance. However, contrary to the usual inverse transformation algorithms, here, the only parameter to be adjusted is the time step size. This parameter is determined with respect to the wave speed and the spatial mesh size. Hence, it depends only on physical values and not on some sophisticated parameters as in usual numerical inverse transformation formulas.

Acknowledgement The author gratefully acknowledges the financial support by the Austrian Science Fund (FWF) under grant P18481-N13. The fruitful and helpful discussion with L. Banjai and S. Sauter during the author's stay at the University of Zürich is as well gratefully acknowledged.

References

[1] A. I. Abreu, J. A. M. Carrer, and W. J. Mansur. Scalar wave propagation in 2D: a BEM formulation based on the operational quadrature method. *Eng. Anal. Bound. Elem.*, 27: 101–105, 2003.

[2] A. I. Abreu, W. J. Mansur, and J. A. M. Carrer. Initial conditions contribution in a BEM formulation based on the convolution quadrature method. *Int. J. Numer. Methods. Engrg.*, 67:417–434, 2006.

[3] S. Ahmad and G. D. Manolis. Dynamic analysis of 3-D structures by a transformed boundary element method. *Comput. Mech.*, 2:185–196, 1987.

[4] H. Antes. A boundary element procedure for transient wave propagations in two-dimensional isotropic elastic media. *Finite Elements in Analysis and Design*, 1:313–322, 1985.

[5] H. Antes and M. Jäger. On stability and efficiency of 3d acoustic BE procedures for moving noise sources. In S.N. Atluri, G. Yagawa, and T.A. Cruse, editors, *Computational Mechanics, Theory and Applications*, volume 2, pages 3056–3061, Heidelberg, 1995. Springer-Verlag.

[6] L. Banjai and S. Sauter. Rapid solution of the wave equation in unbounded domains. *SIAM J. Numer. Anal.*, 47(1):227–249, 2009.

[7] D. E. Beskos. Boundary element methods in dynamic analysis. *AMR*, 40(1):1–23, 1987.

[8] D. E. Beskos. Boundary element methods in dynamic analysis: Part II (1986-1996). *AMR*, 50(3):149–197, 1997.

[9] T. A. Cruse and F. J. Rizzo. A direct formulation and numerical solution of the general transient elastodynamic problem, I. *Aust. J. Math. Anal. Appl.*, 22(1):244–259, 1968.

[10] J. Domínguez. *Boundary Elements in Dynamics*. Computational Mechanics Publication, Southampton, 1993.

[11] J. Domínguez. Dynamic stiffness of rectangular foundations. Report no. R78-20, Department of Civil Engineering, MIT, Cambridge MA, 1978.

[12] S. Erichsen and S. A. Sauter. Efficient automatic quadrature in 3-d Galerkin BEM. *Comput. Methods Appl. Mech. Engrg.*, 157(3–4):215–224, 1998.

[13] F. García-Sánchez, Ch. Zhang, and A. Sáez. 2-d transient dynamic analysis of cracked piezoelectric solids by a time-domain BEM. *Comput. Methods Appl. Mech. Engrg.*, 197 (33-40):3108–3121, 2008.

[14] L. Gaul and M. Schanz. A comparative study of three boundary element approaches to calculate the transient response of viscoelastic solids with unbounded domains. *Comput. Methods Appl. Mech. Engrg.*, 179(1-2):111–123, 1999.

[15] K. F. Graff. *Wave Motion in Elastic Solids*. Oxford University Press, 1975.

[16] M. Guiggiani and A. Gigante. A general algorithm for multidimensional cauchy principal value integrals in the boundary element method. *J. of Appl. Mech.*, 57:906–915, 1990.

[17] W. Hackbusch, W. Kress, and S. A. Sauter. Sparse convolution quadrature for time domain boundary integral formulations of the wave equation by cutoff and panel-clustering. In M. Schanz and O. Steinbach, editors, *Boundary Element Analysis: Mathematical Aspects and Applications*, volume 29 of *Lecture Notes in Applied and Computational Mechanics*, pages 113–134. Springer-Verlag, Berlin Heidelberg, 2007.

[18] E. Kausel. *Fundamental Solutions in Elastodynamics*. Cambridge University Press, 2006.

[19] L. Kielhorn and M. Schanz. Convolution quadrature method based symmetric Galerkin boundary element method for 3-d elastodynamics. *Int. J. Numer. Methods. Engrg.*, 76(11): 1724–1746, 2008.

[20] Y. K. Kim and H. B. Kingsbury. Dynamic characterization of poroelastic materials. *Exp. Mech.*, 19(7):252–258, 1979.

[21] C. Lubich. Convolution quadrature and discretized operational calculus. I. *Numer. Math.*, 52(2):129–145, 1988.

[22] C. Lubich. Convolution quadrature and discretized operational calculus. II. *Numer. Math.*, 52(4):413–425, 1988.

[23] Ch. Lubich. Convolution quadrature revisited. *BIT Num. Math.*, 44(3):503–514, 2004.

[24] Ch. Lubich. On the multistep time discretization of linear initial-boundary value problems and their boundary integral equations. *Numer. Math.*, 67:365–389, 1994.

[25] Ch. Lubich and R. Schneider. Time discretization of parabolic boundary integral equations. *Numer. Math.*, 63:455–481, 1992.

[26] G. D. Manolis. A comparative study on three boundary element method approaches to problems in elastodynamics. *Int. J. Numer. Methods. Engrg.*, 19:73–91, 1983.

[27] W. J. Mansur. *A Time-Stepping Technique to Solve Wave Propagation Problems Using the Boundary Element Method*. Phd thesis, University of Southampton, 1983.

[28] W. J. Mansur, J. A. M. Carrer, and E. F. N. Siqueira. Time discontinuous linear traction approximation in time-domain BEM scalar wave propagation. *Int. J. Numer. Methods. Engrg.*, 42(4):667–683, 1998.

[29] G. V. Narayanan and D. E. Beskos. Numerical operational methods for time-dependent linear problems. *Int. J. Numer. Methods. Engrg.*, 18:1829–1854, 1982.

[30] D. Nardini and C. A. Brebbia. A new approach to free vibration analysis using boundary elements. In C. A. Brebbia, editor, *Boundary Element Methods*, pages 312–326. Springer-Verlag, Berlin, 1982.

[31] P. W. Partridge, C. A. Brebbia, and L. C. Wrobel. *The Dual Reciprocity Boundary Element Method*. Computational Mechanics Publication, Southampton, 1992.

[32] A. Peirce and E. Siebrits. Stability analysis and design of time-stepping schemes for general elastodynamic boundary element models. *Int. J. Numer. Methods. Engrg.*, 40(2):319–342, 1997.

[33] D. C. Rizos and D. L. Karabalis. An advanced direct time domain BEM formulation for general 3-D elastodynamic problems. *Comput. Mech.*, 15:249–269, 1994.

[34] M. Schanz. Application of 3-d Boundary Element formulation to wave propagation in poroelastic solids. *Eng. Anal. Bound. Elem.*, 25(4-5):363–376, 2001.

[35] M. Schanz. *Wave Propagation in Viscoelastic and Poroelastic Continua: A Boundary Element Approach*, volume 2 of *Lecture Notes in Applied Mechanics*. Springer-Verlag, Berlin, Heidelberg, New York, 2001.

[36] M. Schanz. Storage reduced poroelastodynamic boundary element formulation in time domain. In H. I. Ling, A. Smyth, and R. Betti, editors, *Poromechanics IV*, pages 902–907, Lancaster, 2009. DEStech Publications, Inc.

[37] M. Schanz and H. Antes. Application of 'operational quadrature methods' in time domain boundary element methods. *Meccanica*, 32(3):179–186, 1997.

[38] M. Schanz and H. Antes. A new visco- and elastodynamic time domain boundary element formulation. *Comput. Mech.*, 20(5):452–459, 1997.

[39] M. Schanz and L. Kielhorn. Dimensionless variables in a poroelastodynamic time domain boundary element formulation. *Building Research Journal*, 53(2-3):175–189, 2005.

[40] O. Steinbach. *Numerical Approximation Methods for Elliptic Boundary Value Problems*, volume 54 of *Texts in Applied Mathematics*. Springer, 2008.

[41] L. T. Wheeler and E. Sternberg. Some theorems in classical elastodynamics. *Arch. Rational Mech. Anal.*, 31:51–90, 1968.

[42] G. Yu, W. J. Mansur, J. A. M. Carrer, and L. Gong. Time weighting in time domain BEM. *Eng. Anal. Bound. Elem.*, 22(3):175–181, 1998.

[43] G. Yu, W. J. Mansur, J. A. M. Carrer, and L. Gong. Stability of Galerkin and Collocation time domain boundary element methods as applied to the scalar wave equation. *Comput. & Structures*, 74(4):495–506, 2000.

[44] Ch. Zhang. Transient elastodynamic antiplane crack analysis in anisotropic solids. *Internat. J. Solids Structures*, 37(42):6107–6130, 2000.